Small divergence edge-emitting semiconductor lasers with two-dimensional plasmonic collimators

Nanfang Yu, Romain Blanchard, Jonathan Fan, Federico Capasso, Tadataka Edamura, Masamichi Yamanishi, and Hirofumi Kan

Citation: Appl. Phys. Lett. **93**, 181101 (2008); doi: 10.1063/1.3009599
View online: https://doi.org/10.1063/1.3009599
View Table of Contents: http://aip.scitation.org/toc/apl/93/18
Published by the American Institute of Physics

Small divergence edge-emitting semiconductor lasers with two-dimensional plasmonic collimators

Nanfang Yu,[1,a)] Romain Blanchard,[1] Jonathan Fan,[1] Federico Capasso,[1,b)] Tadataka Edamura,[2] Masamichi Yamanishi,[2] and Hirofumi Kan[2]
[1]*School of Engineering and Applied Sciences, Harvard University, Cambridge, Massachusetts 02138, USA*
[2]*Central Research Laboratory, Hamamatsu Photonics K.K., Hamamatsu 434-8601, Japan*

(Received 21 July 2008; accepted 18 September 2008; published online 3 November 2008)

Using quantum cascade lasers with a two-dimensional metallic aperture-grating structure defined on the facet the authors demonstrate a collimated laser beam with small divergence angle perpendicular and parallel to the laser waveguide layers (2.7° and 3.7°, respectively). These values represent a reduction by a factor of ~30 and ~10, respectively, compared to those of the original 8.06-μm-wavelength laser without plasmonic collimation. The devices preserve good room temperature performance with output power as high as 53% of that of the original unpatterned lasers. © *2008 American Institute of Physics*. [DOI: 10.1063/1.3009599]

Edge-emitting semiconductor lasers suffer from a large intrinsic beam divergence, caused by their small aperture size. The divergence angle θ of a beam emitted by an aperture of dimension L scales approximately as λ/L, where λ is the free space wavelength. The full width at half maximum (FWHM) divergence angles in directions normal and parallel to the waveguide layers are denoted as $\theta_{\perp}$ and $\theta_{\parallel}$; they typically range from 30° to 80° and from 20° to 60°, respectively, for edge-emitting semiconductor lasers. A much smaller divergence would be invaluable for many applications, such as facilitating coupling of the laser output into optical fibers and waveguides, and free space communication, ranging, and remote sensing.

Lezec *et al.*, demonstrated that a plasmonic aperture-groove structure defined in a suspended metal film can collimate incident light.[1] Since then, there have been a few attempts to integrate this structure with an active device.[2,3] Recently, we demonstrated a very small beam divergence in the laser polarization direction for quantum cascade lasers (QCLs) by patterning the facet with a suitable metallic structure consisting of an aperture and an adjacent one dimensional (1D) grating.[4] In this letter, we extend this idea and show that by defining a plasmonic two-dimensional (2D) pattern on the laser facet, we are able to achieve 2D collimation for linearly-polarized edge-emitting semiconductor lasers. Midinfrared QCLs are used as the model system; the fabricated devices preserved good room temperature performance with an output power as high as 53% of that of the original unpatterned devices.

Our 2D plasmonic collimator consists of a subwavelength aperture opened on the laser active region and an array of half rings centered on the aperture; see Fig. 1(a) for a sketch of the design.

Beam collimation in the fabricated devices is essentially an interference effect: the aperture couples the laser output into surface plasmons (SPs), while the half-ring pattern functions as a 2D ensemble of scatterers that coherently radiate the energy of the SPs into the far field; radiation from the aperture and from the scattered SPs interfere constructively, leading to increased intensity in a small solid angle.

The choice of the size of the aperture results from a trade-off between power outflow and divergence. On the one hand, a large aperture let more power to emerge from the laser cavity. On the other hand, in order to achieve 2D collimation, the aperture needs to be subwavelength so that the SPs propagating along the laser facet have a sufficiently large divergence angle. Collimation in the directions normal and parallel to the laser material layers is only effective if the SPs cover a large distance on the facet in both directions without significant attenuation. An optimal choice of the aperture size will depend on the application envisioned for the devices. We used finite-element simulations (COMSOL Multiphysics) to study the dependence of the device performance on the aperture size. Figure 1(b) shows the evolution of the SP divergence angles (FWHM) with the lateral aperture size [w_1 in Fig. 1(a)] for $\lambda=8.06$ μm devices. The results show that as long as w_1 is smaller than λ, one can get substantial SP diffraction. Figure 1(c) plots the intensity of the SPs for a device with a $w_1 \times w_2 = 4 \times 2$ μm^2 aperture, showing that the SPs are spreading widely on the laser facet. In all the simulations, we kept the vertical aperture size w_2 constant around 2 μm, which is nearly equal to the laser active region thickness. We chose not to enlarge w_2 because the laser mode is confined in the active core with a cross section of 2.1×9.7 μm^2 in the vertical and lateral directions. w_2 larger than the active region thickness will quickly reduce the efficiency of coupling into SPs because it reduces the overlapping between the laser mode and the edges of the aperture.

The plasmonic pattern was chosen to be ringlike in order to match its shape to the SP wavefront. Simulations confirmed that for the aperture shape and size considered (rectangular with w_1 between 2 and 10 μm and $w_2=2$ μm), the SP wavefront is approximately circular [for instance, see Fig. 1(c)]. The period of the rings was designed to match the SP wavelength of the patterned metal surface (second order grating) so that the collimated beam is normal to the laser facet in the far field in a manner analogous to the 1D plasmonic collimation.[4] It is preferable to have as many rings as possible in order to concentrate light into a smaller solid angle. The limiting factor is the propagation distance of SPs whose

a)Electronic mail: nyu@fas.harvard.edu.
b)Author to whom correspondence should be addressed. Electronic mail: capasso@seas.harvard.edu.

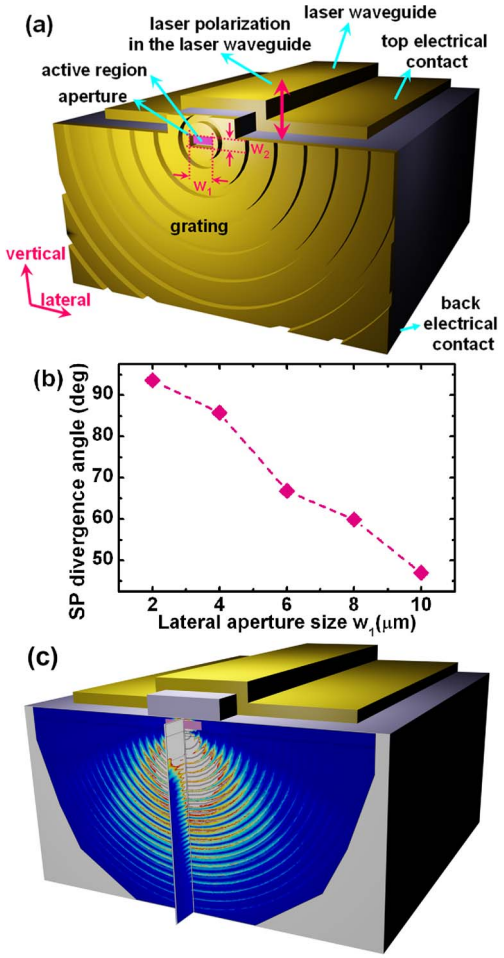

FIG. 1. (Color online) (a) A sketch of the device, consisting of a QCL and a metallic aperture-grating structure defined on its facet. (b) Simulated FWHM divergence angle of SPs as a function of the lateral aperture size w_1. The vertical aperture size w_2 is kept constant at 2 μm. (c) Simulated electric-field intensity $|E|^2$ on the facet. Two "slice views" of the intensity are represented: one parallel to the laser facet, 100 nm above the interface (the half-intensity decay length of SPs is approximately 3 μm away from the facet), the other perpendicular to the laser facet, in the symmetry plane along the laser ridge.

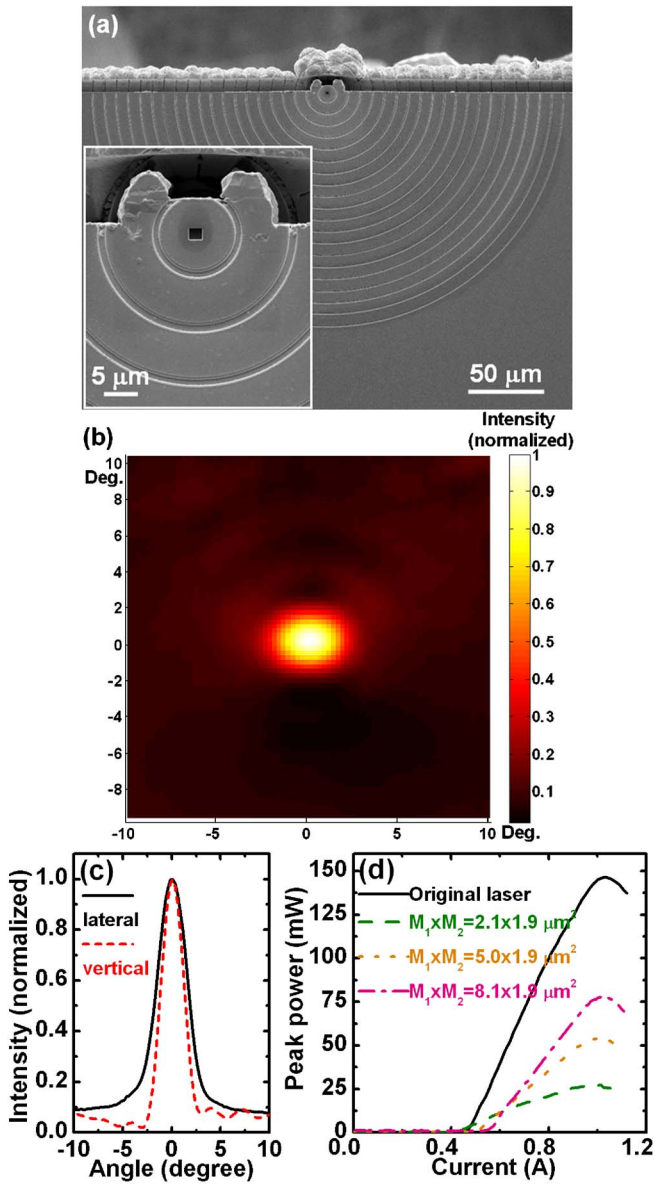

FIG. 2. (Color online) Experimental results of a representative BHT QCL with the plasmonic collimator. (a) An electron micrograph of the device facet patterned with 20 rings. The rings are 0.6-μm wide and 1.0-μm deep, with a periodicity of 7.8 μm. The radius of the first ring is 6.0 μm. The inset is a zoom-in view of the facet. Aperture size $w_1 \times w_2 = 2.1 \times 1.9$ μm^2. (b) Measured 2D far-field intensity distributions for the device at I_{dr} =600 mA. (c) Line scans of (b) in the vertical and lateral directions. (d) Light output vs current characteristics taken for the device before and after defining the plasmonic collimator. In all the measurements, the lasers are operated at room temperature in pulsed mode with an 80 kHz repetition rate and 125 ns pulse duration.

energy is dissipated by heat generation in the metal and scattering by the surface roughness and the grating grooves. At midinfrared wavelengths, SPs are able to propagate over a few hundreds of microns,[5] which allows us to fabricate up to tens of rings. We performed simulations to adjust the ring width and depth to maximize the intensity of the collimated beam. The diameter of the first ring r_1 was tuned to achieve maximum constructive interference between the beam directly emerging from the aperture and the ones scattered by the ring grooves. Since the complete understanding of the field in the near zone around a metallic aperture is still subjected to debate,[6–8] we used simulations to help determine r_1. A list of the optimized design parameters, including grating period, width and depth of grooves, and radius of the first ring groove, is presented in the caption of Fig. 2.

To fabricate the devices, first focus ion beam (FIB) milling was used to define ring grooves in the semiconductor; second a 200-nm-thick alumina film was deposited onto the laser facet for electrical insulation, followed by deposition of a 600-nm-thick gold film; finally FIB milling was used again to open the aperture by removing a piece of gold film in front of the laser active region. Multiangle deposition was implemented such that the walls of the grooves are also covered by alumina and gold films. We report experimental and simulation results demonstrating 2D collimation for buried heterostructure (BHT) $\lambda = 8.06$ μm QCLs grown by metal organic vapor-phase epitaxy.[9]

Systematic experiments were performed to study the evolution of the beam divergence angles $\theta_\perp$ and $\theta_\parallel$ and the output power as the lateral aperture size w_1 is enlarged in steps using FIB milling. An electron micrograph of the facet of a representative device is shown in Fig. 2(a). It was patterned with 20 rings and the aperture size $w_1 \times w_2$ is approximately 2.1×1.9 μm^2. The measured far-field intensity distributions, Fig. 2(b), show that the device has divergence

angles $\theta_\perp$ and $\theta_\parallel$ equal to 2.7° and 3.7°, respectively. These are substantial reduction in the beam divergence in comparison to that of the original devices with unpatterned facet: $\theta_\perp=74°$ and $\theta_\parallel=42°$. To evidence the role of the collimation grating, simulations were performed showing that $\theta_{\perp=}128°$ and $\theta_\parallel=104°$ for a structure with just a 2.1×1.9 μm^2 aperture and without any grating. Our far-field measurement setup is described in Ref. 4. It is observed from Fig. 2(c), the line scans of Fig. 2(b), that the level of the optical background outside the central beam is less than 10% of the peak intensity of the central beam. As a figure of merit we use the concept of antenna directivity to characterize the collimation of the device. Directivity is defined as $D=10\log_{10}(2\pi I_{peak}/I_{total})$, where I_{peak} is the far-field peak intensity and I_{total} is the total intensity under the 2D far-field beam profile. We calculate based on our experimental results that D is approximately 26.9 dB for the device with 20 rings, while D is only about 8.3 dB for the original unpatterned lasers. The beam quality factor (M^2 factor) of the device is determined to be about 2.0 in both vertical and lateral directions based on measurements on the variation of the beam waist along the propagation direction.

The $\lambda=8.06$ μm BHT devices have multiple longitudinal modes and a higher driving current I_{dr} usually corresponds to a larger laser spectrum width $\Delta\lambda$. For instance, for the device with 20 rings, $\Delta\lambda$ is approximately 0.05 μm at $I_{dr}=500$ mA; $\Delta\lambda$ broadens to about 0.3 μm at $I_{dr}=600$ mA and keeps around 0.3 μm at higher I_{dr}. One would expect that the collimation of the patterned devices will get worse for a broader spectrum because the period of the ring grating is matched only with the central lasing wavelength. However, we found that the far-field divergence angles measured were relatively stable at different driving currents: $\theta_{\perp=}2.6°$ and $\theta_\parallel=3.7°$ for $I_{dr}=500$ mA; $\theta_{\perp=}2.7°$ and $\theta_\parallel=3.7°$ for $I_{dr}=600$ mA. The directivities D at these currents were found to be around 27 dB. These observations demonstrate that the ring collimator design is quite robust with respect to spectral broadening. We are investigating the reasons behind this phenomenon.

As mentioned above, a trade-off needs to be made between the achievable divergence angles and the output power. The device reported in Figs. 2(a)–2(c) with a $w_1\times w_2=2.1\times1.9$ μm^2 aperture and 20 rings have desirable far-field performance but its power output is only around 20% of that of the original device [Fig. 2(d)]. We proceeded to increase w_1 to 5.0 μm and eventually to 8.1 μm to boost the power throughput; the corresponding maximum output power of the device was increased to 37% and 53% of that of the original laser; see Fig. 2(d) for the measured light output versus current characteristics. The counterpart of the increased output power is the broadening of the central beam in the lateral direction due to the narrowing of the SP divergence on the laser facet. We found that $\theta_\perp$ and $\theta_\parallel$ follow a trend in good agreement with our simulation results (Fig. 3):

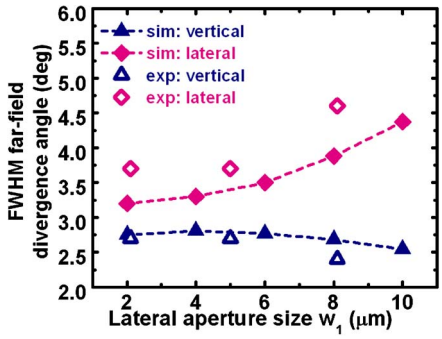

FIG. 3. (Color online) Divergence angles in directions perpendicular and parallel to the laser material layers as a function of the lateral aperture size w_1. Calculation results are represented with filled symbols and experimental results are represented with hollow symbols.

with an increasing w_1, $\theta_\perp$ increases first slowly and then relatively fast while $\theta_\parallel$ is nearly a constant. For instance, $\theta_\perp$ equals to 2.7°, 2.7°, and 2.4°, $\theta_\parallel$ equals to 3.7°, 3.7°, and 4.6° when w_1 was increased from 2.1 to 5.0, and finally to 8.1 μm.

In conclusion, we have performed systematic experiments and simulations to demonstrate that the integration of a suitably designed 2D aperture-grating structure on the facet of QCLs reduces the beam divergence angles by a factor up to ~30 and ~10 in the vertical and lateral directions, respectively, down to 2.7° and 3.7°. The fabricated devices preserve a significant output power. We plan to investigate optimized aperture shapes to enhance the output power and extend the concept of plasmonic collimation to visible and near-infrared edge-emitting laser diodes and VCSELs.

We acknowledge support from the Air Force Office of Scientific Research (AFOSR MURI on Plasmonics) and the Harvard Nanoscale Science and Engineering Center (NSEC). This work was performed in part at the Center for Nanoscale Systems (CNS) at Harvard University, a member of the National Nanotechnology Infrastructure Network (NNIN), which is supported by the National Science Foundation under NSF Award No. ECS-0335765. CNS is part of the Faculty of Arts and Sciences at Harvard University.

[1] H. J. Lezec, A. Degiron, E. Devaux, R. A. Linke, L. Martín-Moreno, F. J. García-Vidal, and T. W. Ebbesen, Science **297**, 820 (2002).
[2] B. Guo, G. Song, and L. Chen, Appl. Phys. Lett. **91**, 021103 (2007).
[3] J. Gao, G. Song, Q. Gan, B. Guo, and L. Chen, Laser Phys. Lett. **4**, 234 (2007).
[4] N. Yu, J. Fan, Q. J. Wang, C. Pflügl, L. Diehl, T. Edamura, M. Yamanishi, H. Kan, and F. Capasso, Nat. Photonics **2**, 564 (2008).
[5] L. Novotny and B. Hecht, *Principles of Nano-Optics* (Cambridge University Press, Cambridge, 2006).
[6] G. Gay, O. Alloschery, B. Viaris De Lesegno, C. O'Dwyer, J. Weiner, and H. J. Lezec, Nat. Phys. **2**, 262 (2006).
[7] G. Lévêque and O. J. F. Martin, Phys. Rev. B **76**, 155418 (2007).
[8] P. Lalanne and J. P. Hugonin, Nat. Phys. **2**, 551 (2006).
[9] K. Fujita, S. Furuta, A. Sugiyama, T. Ochiai, T. Edamura, N. Akikusa, M. Yamanishi, and H. Kan, Appl. Phys. Lett. **91**, 141121 (2007).